2003

Isomerization of the Newly Discovered Interstellar Molecule SiCN to SiNC Through Two Transition States

Nancy A. Richardson
Liberty University, narichardson@liberty.edu

Isomerization of the interstellar molecule silicon cyanide to silicon isocyanide through two transition states

Nancy A. Richardson[a)]
Department of Basic Sciences and Engineering, Pensacola Christian College, Pensacola, Florida 32503

Yukio Yamaguchi and Henry F. Schaefer III[b)]
Center for Computational Chemistry, University of Georgia, Athens, Georgia 30602

(Received 8 September 2003; accepted 29 September 2003)

A range of highly correlated *ab initio* methods is used to predict the geometrical parameters of silicon cyanide (SiCN), silicon isocyanide (SiNC), and two transition states ($^2A'$ and $^2A''$) for the isomerization reaction transforming one to the other. Also predicted are dipole moments, rotational constants, and harmonic vibrational frequencies. At all levels of theory, the SiCN and SiNC molecules are predicted to have linear equilibrium structures. The SiNC isomer is found to lie 1.5 kcal/mol above the SiCN species at the coupled cluster (CC) with single, double, and full triple excitations (CCSDT) level of theory with the correlation-consistent polarized valence quadruple zeta (cc-pVQZ) basis set. These theoretical predictions complement the recent laboratory production of SiCN and SiNC and subsequent astronomical detection of SiCN in the envelope of the C Star IRC+10216/CW Leo. The theoretical B_e values of 5481 MHz (SiCN) and 6316 MHz (SiNC) at the CC with single, double, and iterative partial triple excitations (CCSDT-3) level of theory with the cc-pVQZ basis set are consistent with the experimental B_0 values of 5543 MHz (SiCN) and 6397 MHz (SiNC). The transition states for the isomerization reaction SiCN→SiCN are found to proceed through the $^2A'$ and $^2A''$ surfaces, which lie 20.9 and 21.8 kcal/mol above the SiCN minimum at the cc-pVQZ CCSDT-3 level of theory. The ground states of SiCN and SiNC radicals are subject to Renner–Teller interactions. At the CC with single, double, and perturbative triple excitations [CCSD(T)] level of theory, the Renner parameters and the averaged harmonic bending vibrational frequencies are determined to be 0.318 and 249 cm^{-1} for SiCN and 0.412 and 195 cm^{-1} for SiNC.
 [DOI: 10.1063/1.1627290]

I. INTRODUCTION

Silicon containing molecules are found in interstellar space and in some stars. One such occurrence, reported in 1986, was the observation of a radical in the envelope of a carbon star.[1] The molecule is linear or slightly asymmetric and must have an odd number of electrons. The rotational constant was found to be 5966.8 MHz. The most likely candidates for such a radical are HSiCC, SiCCH, HSCC, silicon cyanide (SiCN), and silicon isocyanide (SiNC). Subsequent theoretical investigations by Largo-Cabrerizo and coworkers showed that the astronomical observations could not be explained by assigning the spectra to HSiCC,[2] SiCCH,[2] SiCN,[3] or SiNC.[3] In 2000, Apponi *et al.*[4,5] reported the radio spectra of SiCCH, SiCN, and SiNC. These three silicon-bearing radicals of astrophysical interest were detected in a laboratory discharge in their $\tilde{X}\,^2\Pi$ ground states by Fourier transform microwave and millimeter-wave absorption spectroscopy.[4,5] With the availability of precise microwave spectra for these molecules, Guélin *et al.*[6] subsequently reported the detection of the SiCN radical in an astronomical source, the envelope of the C star IRC+10216/CW Leo.

As mentioned above, Largo-Cabrerizo carried out a theoretical study of the SiCN and SiNC radicals.[3] He used the unrestricted Hartree–Fock (UHF) 6-31G(d) method to locate stationary points. With fourth-order Møller–Plesset perturbation [MP4(SDTQ)] theory with a valence triple zeta + single polarization basis set [MC-311G(d)] he predicted that SiCN lies 1.9 kcal/mol above SiCN. The barrier for the isomerization reaction (SiNC→SiCN) was estimated to be 18.2 kcal/mol relative to the SiNC isomer with the MP2/6-31G(d)//UHF/6-31G(d) method. It should be pointed out that Largo-Cabrerizo located the transition state only on the $^2A''$ surface.

In this work, a series of *ab initio* methods including self-consistent field (SCF), configuration interaction with single and double excitations (CISD), coupled cluster (CC) with single and double excitations (CCSD),[7,8] CCSD with perturbative triple excitations [CCSD(T)],[9,10] CC with single, double, and iterative partial triple excitations (CCSDT-3)[11] will be used to determine the geometries, dipole moments, rotational constants, harmonic vibrational frequencies, and energetics of SiCN and SiNC, as well as the barriers to isomerization from SiCN to SiNC. In order to energetically confirm the global minimum of the SiCN–SiNC system, CC with single, double, and full triple excitations (CCSDT)[12–14] level of theory will be employed as well.

[a)]Also at: Center for Computational Chemistry, University of Georgia, Athens, Georgia 30602.
[b)]Electronic mail: hfsiii@uga.edu

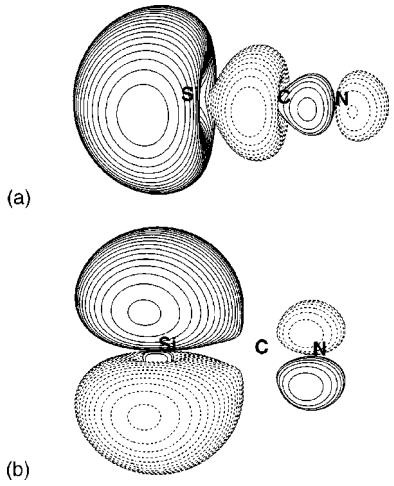

FIG. 1. (a) The 9σ molecular orbital for the $\tilde{X}\,^2\Pi$ state of SiCN from the TZ2PF SCF method. (b) The 3π molecular orbital for the $\tilde{X}\,^2\Pi$ state of SiCN from the TZ2PF SCF method.

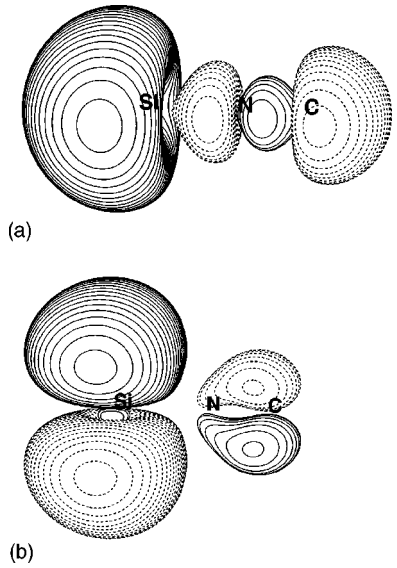

FIG. 2. (a) The 9σ molecular orbital for the $\tilde{X}\,^2\Pi$ state of SiNC from the TZ2PF SCF method. (b) The 3π molecular orbital for the $\tilde{X}\,^2\Pi$ state of SiNC from the TZ2PF SCF method.

II. ELECTRONIC STRUCTURE CONSIDERATIONS

SiCN and SiNC radicals belong to the family of 13 valence electron systems. According to Walsh rules,[15] such triatomic molecules are expected to have linear structures in their electronic ground states and are indeed found to be linear theoretically[3] and experimentally.[4–6] The SiCN species is a Renner–Teller molecule[16–25] with electron configuration

$$[\text{core}](6\sigma)^2(7\sigma)^2(8\sigma)^2(2\pi_y)^2(2\pi_x)^2(9\sigma)^2(3\pi_y), \qquad (1)$$

for its $\tilde{X}\,^2\Pi$ electronic ground state. In Eq. (1) [core] denotes the seven lowest-lying core orbitals. The π_y and π_x components refer to *yz* plane and *xz* plane π orbitals (the *z* axis is assigned to the molecular axis). The single occupation of $3\pi_y$ removes the degeneracy of the bending mode, since *yz* plane and *xz* plane bendings perturb singly occupied and unoccupied orbitals. The 6σ orbital is the σ bond between carbon and nitrogen. 7σ represents the σ bond between silicon and carbon composed of the 3*s* orbital of silicon and the 2*p* orbital of carbon. The 8σ orbital is antibonding between carbon and silicon. More electron density resides on the outermost atoms, giving 8σ considerable lone-pair character. The 9σ orbital depicted in Fig. 1(a) has lone-pair character on silicon and a smaller amount of electron density on nitrogen with a carbon–nitrogen bond in between. The 2π orbital is a CN π bonding orbital, while the 3π orbital shown in Fig. 1(b) is a weak SiC π bonding orbital (almost Si 3*p*-like nonbonding orbital). The electronegativities[26] of the C (2.5) and N (3.0) atoms are larger than that of the Si (1.8) atom. Therefore, the contribution of C and N 2*p* orbitals is greater for the bonding 2π orbital, while the contribution of the Si 3*p* orbital is dominant for the weak π bonding (almost nonbonding) 3π orbital.

The SiNC radical is also a Renner–Teller molecule[16–25] and has an $\tilde{X}\,^2\Pi$ electronic ground state

$$[\text{core}](6\sigma)^2(7\sigma)^2(2\pi_y)^2(2\pi_x)^2(8\sigma)^2(9\sigma)^2(3\pi_y). \qquad (2)$$

The orbital ordering in SiNC is similar to SiCN except for the 2π and 8σ orbitals which are oppositely ordered in the isomers. 8σ is an antibonding orbital between carbon and nitrogen. More electron density resides on the outermost atom. The 9σ orbital represented in Fig. 2(a) has lone-pair character on silicon and some amount of electron density on carbon with a nitrogen–carbon bond in between. The 2π orbital is an NC π bonding orbital, whereas the 3π orbital shown in Fig. 2(b) is a weak SiN π bonding orbital (almost Si 3*p*-like nonbonding orbital). Since the SiCN and SiNC radicals have two distinct *real* bending vibrational frequencies, they may be classified as type A Renner–Teller molecules following the analyses for linear triatomic molecules by Lee *et al.*[22]

The electron configuration of the transition state on the $^2A'$ surface is

$$[\text{core}](7a')^2(8a')^2(9a')^2(2a'')^2(10a')^2(11a')^2(12a'), \qquad (3)$$

where $12a'$ corresponds to the in-plane $3\pi_y$ orbital in the linear configuration. The transition state on the $^2A''$ surface has the electronic arrangement

$$[\text{core}](7a')^2(8a')^2(9a')^2(2a'')^2(10a')^2(11a')^2(3a''), \qquad (4)$$

where $3a''$ corresponds to the out-of-plane $3\pi_x$ orbital in the linear configuration.

For open-shell systems, it is helpful to analyze the molecular orbital (MO) Hessian of the reference SCF wave functions. The MO Hessian is defined as the second derivatives of the SCF energy with respect to independent MO rotations. The signs and magnitudes of the eigenvalues for the MO Hessian provide useful information concerning the instability of SCF wave functions.[27–29] At the linear configuration, the MO Hessian matrix for the $\tilde{X}\,^2\Pi$ state of SiCN has one zero eigenvalue. The eigenvector of the zero eigen-

value is associated with a $3\pi_y - 3\pi_x$ MO rotation. Therefore, an exchange of two MOs does not alter the SCF energy. Similarly, the $\tilde{X}\,^2\Pi$ state of linear SiNC has one zero eigenvalue for the MO Hessian. The eigenvector of the zero eigenvalue is again related to a $3\pi_y - 3\pi_x$ MO rotation.

At the isomerization transition state on the $^2A'$ potential energy surface, the MO Hessian has one negative eigenvalue whose eigenvector is associated with a $12a' - 3a''$ MO rotation. Thus, the SCF wave function is *unstable* and there exists a lower-lying electronic state ($^2A''$) at the $^2A'$ transition state geometry. On the other hand, the MO Hessian at the transition state on the $^2A''$ surface has also one negative eigenvalue whose eigenvector is related to a $3a'' - 12a'$ MO rotation. Consequently, the SCF wave function at the $^2A''$ transition state is *unstable* and there is a lower-lying electronic state ($^2A'$). This peculiar (relative to equilibrium geometries) situation is due to the fact that each transition state lies at the top of its respective minimum energy path. Although the reference SCF wave functions at their respective transition states are unstable, energetics, and physical properties including dipole moments and harmonic vibrational frequencies at the correlated levels of theory should be correctly determined without variational collapse due to the spatial orthogonality of wave functions.

III. RENNER–TELLER INTERACTIONS

The $\tilde{X}\,^2\Pi$ states of SiCN and SiNC, respectively, present two distinct *real* vibrational frequencies along the bending coordinates. In other words, these two isomers are subject to the Renner–Teller interaction.[16–25] Referring to the arguments given in Ref. 19, the zeroth-order bending potential function may be written as the mean of the V^+ and V^- potentials, neglecting anharmonic terms, as

$$V^0 = \frac{V^+ + V^-}{2} = ar^2, \tag{5}$$

where a is the mean force constant. The Renner–Teller splitting is defined as

$$V = V^+ - V^- = \alpha r^2, \tag{6}$$

where α is the force constant for the splitting function and its sign is dependent on whether the V^+ surface lies above or below the V^- surface. The Renner parameter, ϵ, is a dimensionless constant used to describe the Renner–Teller splitting of the bending potential and is defined as

$$\epsilon = \frac{V^+ - V^-}{V^+ + V^-} = \frac{\alpha}{2a}, \tag{7}$$

which is equivalent to

$$\epsilon = \frac{f^+ - f^-}{f^+ - f^-}, \tag{8}$$

where f^+ and f^- denote the force constants associated with the two distinct bending modes. The Renner parameter may be reexpressed using the two bending frequencies as

$$\epsilon = \frac{(\omega^+)^2 - (\omega^-)^2}{(\omega^+)^2 + (\omega^-)^2}. \tag{9}$$

The actual bending mode observed experimentally is a combination of the ω_2^+ and ω_2^- modes and is determined for the zeroth-order bending potential

$$\tilde{\omega}_2 = \frac{1}{2\pi c}\sqrt{\frac{a}{\mu}} = \frac{1}{2\pi c}\sqrt{\frac{f^+ + f^-}{2\mu}}, \tag{10}$$

where a is the mean force constant defined by Eq. (5) and μ is the kinetic energy contribution of the bending motion. This equation for the averaged bending frequency may be rewritten as

$$\tilde{\omega}_2 = \sqrt{\frac{1}{2}[(\omega^+)^2 + (\omega^-)^2]}. \tag{11}$$

Using Eqs. (5)–(11), the parameters associated with the Renner–Teller interaction may be determined theoretically, in a manner completely independent of the experimental quantities.

IV. THEORETICAL PROCEDURES

Four basis sets were used in this study. The triple ζ (TZ) basis sets for C and N are Dunning's triple-ζ contraction[30] of Huzinaga's primitive Gaussian set[31] and are designated $(10s6p/5s3p)$. The TZ basis set for Si is derived from McLean and Chandler's contraction[32] of Huzinaga's primitive Gaussian set[33] and is designated $(12s9p/6s5p)$. The orbital exponents of the polarization functions are: $\alpha_d(\mathrm{C}) = 1.50$ and 0.375, $\alpha_d(\mathrm{N}) = 1.60$ and 0.40, and $\alpha_d(\mathrm{Si}) = 1.00$ and 0.25 for double polarization (TZ2P). The orbital exponents of the higher angular momentum functions are: $\alpha_f(\mathrm{C}) = 0.80$, $\alpha_f(\mathrm{N}) = 1.00$, and $\alpha_f(\mathrm{Si}) = 0.32$ for one set of higher angular momentum functions (TZ2PF). The correlation consistent polarized valence triple-ζ (cc-pVTZ) and quadruple-ζ (cc-pVQZ) basis sets are those developed more recently by Dunning and co-workers.[34,35]

The zeroth-order descriptions of all stationary points were obtained using single configuration SCF (restricted open-shell Hartree–Fock) wave functions. Correlation effects were included using CISD, CCSD,[7,8] CCSD(T),[9,10] CCSDT-3,[11] and CCSDT[12–14] levels of theory. In the correlated procedures, the seven lowest-lying core (Si $1s$-, $2s$-, $2p$-like and C, N $1s$-like) orbitals were frozen and three highest-lying virtual (Si, C, N $1s^*$-like) orbitals were deleted for the two TZ plus basis sets, and the seven lowest-lying core orbitals were frozen for the two correlation-consistent basis sets. The cc-pVQZ CISD wave functions of the $\tilde{X}\,^2\Pi$ states have 152 286 configuration state functions in C_{2v} symmetry and display configuration interaction coefficients of $C_0 = 0.936$ (SiCN) and $C_0 = 0.938$ (SiNC) for the reference states at the respective equilibrium geometries.

The geometries of all stationary points were optimized via analytic derivative methods[36–38] at the SCF and CISD levels. Harmonic vibrational frequencies at the SCF level were evaluated analytically, while they were determined via finite differences of analytic gradients at the CISD level. In all CC methods, both geometry optimizations and harmonic vibrational frequency calculations were carried out by using five-point numerical differentiation of the total energies. Cartesian forces at optimized geometries were required to be

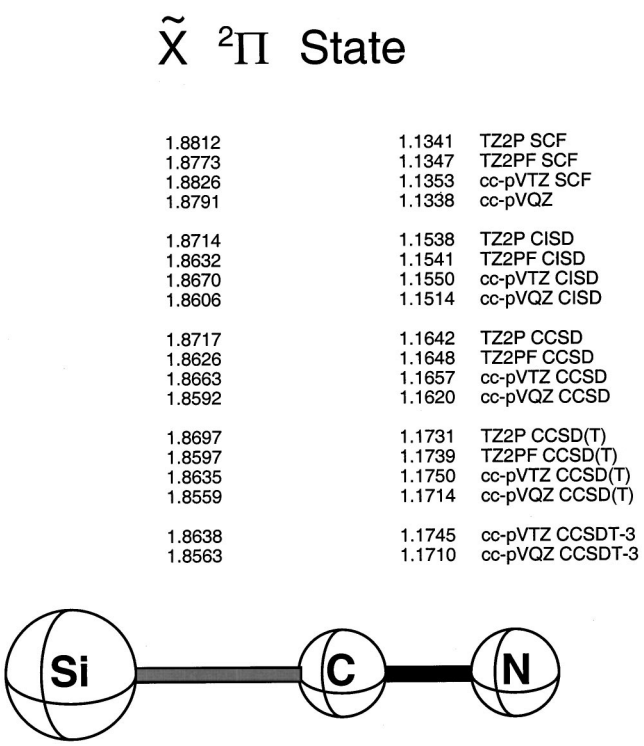

FIG. 3. Predicted geometries for the linear $\tilde{X}\ ^2\Pi$ state of the SiCN molecule. Bond lengths are in Å.

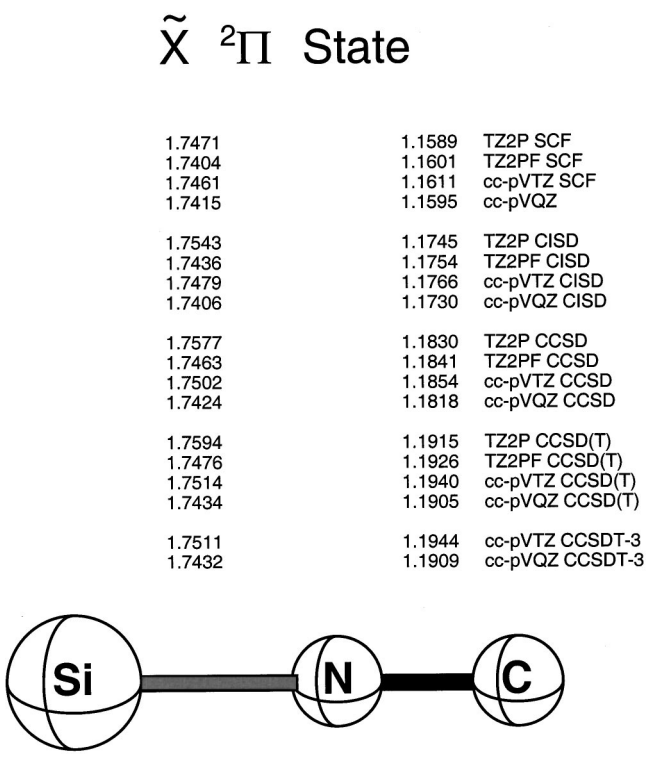

FIG. 4. Predicted geometries for the linear $\tilde{X}\ ^2\Pi$ state of the SiNC molecule. Bond lengths are in Å.

less than 10^{-7} hartree/bohr in all geometry optimizations. Dipole moments were determined as first derivatives of total energies in terms of external electric field. For the CCSD and CCSD(T) methods, dipole moments were evaluated without freezing core/virtual orbitals at the geometries optimized with frozen core/virtual orbitals. For the two equilibrium structures, the zero-point vibrational energies (ZPVEs) are evaluated as

$$(\mathrm{ZPVE})_{\mathrm{eq}} = \tfrac{1}{2}(\omega_1 + 2\tilde{\omega}_2 + \omega_3), \tag{12}$$

and for the two transition state structures, they are determined by

$$(\mathrm{ZPVE})_{\mathrm{ts}} = \tfrac{1}{2}(\omega_1 + \omega_3). \tag{13}$$

All *ab initio* computations were carried out with PSI-2[39] and a local version of the ACESII[40] program on IBM RS/6000 workstations and on our personal computer clusters.

V. RESULTS AND DISCUSSION

In Fig. 3, the optimized structures of the SiCN radical are depicted, while in Fig. 4 those of the SiNC species are shown. The transition state structures on the $^2A'$ and $^2A''$ surfaces are presented in Figs. 5 and 6, respectively. In Tables I–IV, the total energies, dipole moments, harmonic vibrational frequencies, infrared (IR) intensities, and zero-point vibrational energies (ZPVEs) of the four stationary points are presented. The theoretically predicted rotational constants for SiCN and SiNC are compared with the experimentally determined values in Table V. The Renner parameters (ϵ) and averaged bending frequencies ($\tilde{\omega}_2$) are displayed in Table VI. The relative energies for the four stationary points are shown in Table VII.

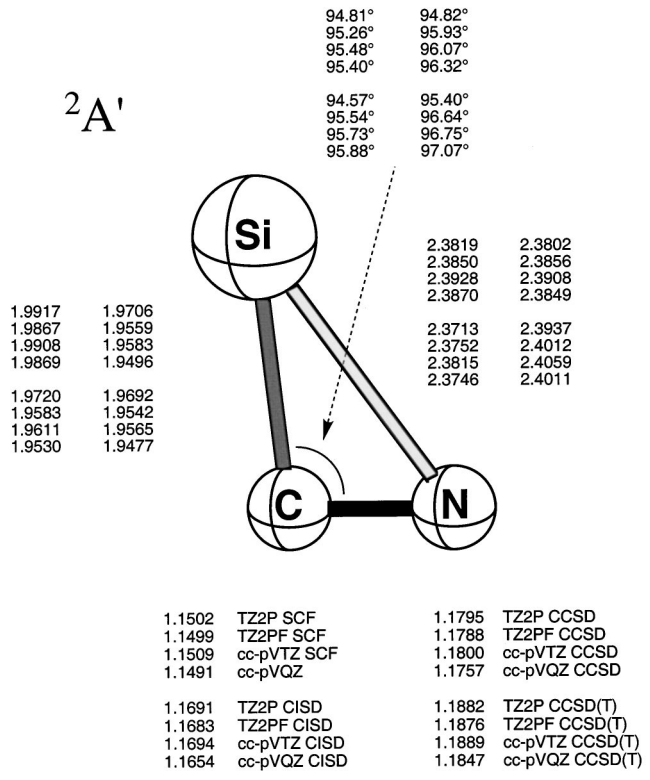

FIG. 5. Predicted geometries for the $^2A'$ transition state for the SiCN↔SiNC isomerization reaction. Bond lengths are in Å.

TABLE I. Theoretical predictions of the total energy (in hartree), dipole moment (in D), harmonic vibrational frequencies (in cm^{-1}), infrared intensities (in parentheses in km mol^{-1}), and ZPVE (in kcal mol^{-1}) for the linear $\tilde{X}\,^2\Pi$ state of SiCN molecule.

Level of theory	Energy	μ_e	$\omega_1(\sigma)$	$\omega_2(\pi^+)$	$\omega_2(\pi^-)$	$\omega_3(\sigma)$	ZPVE
TZ2P SCF	−381.212 681	3.320	2458(15.6)	315(4.6)	238(7.5)	566(97.8)	5.12
TZ2PF SCF	−381.217 021	3.279	2461(15.3)	323(4.7)	245(7.8)	570(97.6)	5.15
cc-pVTZ SCF	−381.218 361	3.255	2459(16.3)	321(4.1)	244(7.2)	568(97.3)	5.14
cc-pVQZ SCF	−381.227 384	3.295	2458(14.8)	319(4.1)	240(7.5)	568(96.9)	5.13
TZ2P CISD	−381.559 596	3.263	2285(22.9)	296(2.8)	222(6.2)	565(80.6)	4.82
TZ2PF CISD	−381.589 212	3.180	2296(20.4)	301(3.1)	224(6.7)	572(78.8)	4.86
cc-pVTZ CISD	−381.594 141	3.122	2294(22.2)	300(2.6)	224(6.0)	573(78.8)	4.86
cc-pVQZ CISD	−381.622 644	⋯	2303(-)	300(-)	220(-)	575(-)	4.87
TZ2P CCSD	−381.603 163	3.282	2185(-)	289(-)	215(-)	558(-)	4.65
TZ2PF CCSD	−381.635 986	3.183	2196(-)	293(-)	216(-)	566(-)	4.68
cc-pVTZ CCSD	−381.641 396	3.098	2194(-)	291(-)	215(-)	567(-)	4.68
cc-pVQZ CCSD	−381.671 973	3.185	2202(-)	291(-)	212(-)	571(-)	4.69
TZ2P CCSD(T)	−381.624 267	3.204	2102(-)	281(-)	205(-)	556(-)	4.50
TZ2PF CCSD(T)	−381.659 396	3.096	2111(-)	289(-)	210(-)	565(-)	4.55
cc-pVTZ CCSD(T)	−381.665 215	2.995	2109(-)	288(-)	205(-)	566(-)	4.54
cc-pVQZ CCSD(T)	−381.697 722	3.090	2116(-)	283(-)	201(-)	569(-)	4.54
cc-pVTZ CCSDT-3	−381.664 065	⋯	⋯	⋯	⋯	⋯	⋯
cc-pVQZ CCSDT-3	−381.696 689	⋯	⋯	⋯	⋯	⋯	⋯
cc-pVTZ CCSDT[a]	−381.665 546	⋯	⋯	⋯	⋯	⋯	⋯
cc-pVQZ CCSDT[a]	−381.697 855	⋯	⋯	⋯	⋯	⋯	⋯

[a]At the CCSD(T) geometries.

A. Geometries

The optimized structures for SiCN are depicted in Fig. 3. For a given basis set, an advanced treatment of correlation effects decreases the SiC bond length and increases the CN bond distance. It is clearly seen that the SCF wave function overestimates the multiple bond character of the CN bond. The optimized structures for SiNC are shown in Fig. 4. Increasingly sophisticated treatments of correlation effects

TABLE II. Theoretical predictions of the total energy (in hartree), dipole moment (in D), harmonic vibrational frequencies (in cm^{-1}), infrared intensities (in parentheses in km mol^{-1}), and ZPVE (in kcal mol^{-1}) for the linear $\tilde{X}\,^2\Pi$ state of SiNC molecule.

Level of theory	Energy	μ_e	$\omega_1(\sigma)$	$\omega_2(\pi^+)$	$\omega_2(\pi^-)$	$\omega_3(\sigma)$	ZPVE
TZ2P SCF	−381.219 016	2.251	2257(506.3)	219(0.04)	146(0.7)	661(156.4)	4.70
TZ2PF SCF	−381.225 141	2.154	2261(511.1)	243(0.05)	177(0.7)	670(153.6)	4.80
cc-pVTZ SCF	−381.226 246	2.200	2259(503.9)	239(0.1)	173(0.7)	667(150.3)	4.78
cc-pVQZ SCF	−381.235 791	2.155	2257(515.2)	237(0.1)	170(0.8)	668(152.5)	4.77
TZ2P CISD	−381.558 479	2.653	2125(329.9)	226(0.1)	148(1.3)	642(124.4)	4.50
TZ2PF CISD	−381.589 602	2.509	2139(330.5)	240(0.1)	165(1.3)	656(120.3)	4.58
cc-pVTZ CISD	−381.594 305	2.522	2137(327.2)	238(0.2)	162(1.4)	656(119.2)	4.58
cc-pVQZ CISD	−381.623 455	⋯	2144(-)	238(-)	159(-)	660(-)	4.59
TZ2P CCSD	−381.599 618	2.811	2049(-)	227(-)	145(-)	631(-)	4.37
TZ2PF CCSD	−381.633 737	2.655	2062(-)	239(-)	159(-)	645(-)	4.45
cc-pVTZ CCSD	−381.638 991	2.641	2061(-)	237(-)	156(-)	646(-)	4.44
cc-pVQZ CCSD	−381.670 216	2.639	2067(-)	238(-)	153(-)	651(-)	4.46
TZ2P CCSD(T)	−381.619 696	2.820	1977(-)	223(-)	142(-)	625(-)	4.25
TZ2PF CCSD(T)	−381.655 957	2.666	1988(-)	237(-)	155(-)	640(-)	4.33
cc-pVTZ CCSD(T)	−381.661 619	2.643	1988(-)	234(-)	153(-)	641(-)	4.32
cc-pVQZ CCSD(T)	−381.694 762	2.652	1992(-)	234(-)	149(-)	645(-)	4.33
cc-pVTZ CCSDT-3	−381.660 872	⋯	⋯	⋯	⋯	⋯	⋯
cc-pVQZ CCSDT-3	−381.694 086	⋯	⋯	⋯	⋯	⋯	⋯
cc-pVTZ CCSDT[a]	−381.662 225	⋯	⋯	⋯	⋯	⋯	⋯
cc-pVQZ CCSDT[a]	−381.695 161	⋯	⋯	⋯	⋯	⋯	⋯

[a]At the CCSD(T) geometries.

TABLE III. Theoretical predictions of the total energy (in hartree), dipole moment (in D), harmonic vibrational frequencies (in cm^{-1}), and ZPVE (in kcal mol^{-1}) for the transition state for the isomerization reaction on the $^2A'$ potential energy surface.

Level of theory	Energy	μ_e	$\omega_1(a')$	$\omega_2(a')$	$\omega_3(a')$	ZPVE
TZ2P SCF	−381.174 219	2.352	2312	372*i*	553	4.09
TZ2PF SCF	−381.177 738	2.314	2319	376*i*	558	4.11
cc-pVTZ SCF	−381.179 703	2.303	2316	376*i*	559	4.11
cc-pVQZ SCF	−381.188 781	2.281	2317	377*i*	556	4.11
TZ2P CISD	−381.522 493	2.292	2147	365*i*	588	3.91
TZ2PF CISD	−381.552 148	2.165	2167	373*i*	604	3.96
cc-pVTZ CISD	−381.557 278	2.122	2165	375*i*	607	3.96
cc-pVQZ CISD	−381.585 895	⋯	2177	378*i*	609	3.98
TZ2P CCSD	−381.566 870	2.328	2052	357*i*	593	3.78
TZ2PF CCSD	−381.599 871	2.182	2073	367*i*	612	3.84
cc-pVTZ CCSD	−381.605 431	2.108	2071	369*i*	615	3.84
cc-pVQZ CCSD	−381.636 167	2.127	2084	374*i*	617	3.86
TZ2P CCSD(T)	−381.589 326	2.275	1973	354*i*	598	3.68
TZ2PF CCSD(T)	−381.624 696	2.128	1995	365*i*	617	3.73
cc-pVTZ CCSD(T)	−381.630 631	2.041	1992	367*i*	620	3.73
cc-pVQZ CCSD(T)	−381.663 364	2.071	2004	373*i*	623	3.76
cc-pVTZ CCSDT-3[a]	−381.629 321	⋯	⋯	⋯	⋯	⋯
cc-pVQZ CCSDT-3[a]	−381.662 170	⋯	⋯	⋯	⋯	⋯
cc-pVTZ CCSDT[a]	−381.630 942	⋯	⋯	⋯	⋯	⋯

[a]At the CCSD(T) geometries.

lengthen both the SiN and NC bond distances. The SiN bond length for SiNC is shorter than the SiC bond length for SiCN at all levels of theory. On the other hand, the NC bond distance for SiNC is longer than the CN bond length for SiCN. The ground state ($X\,^2\Sigma^+$) of the CN radical has an equilibrium bond distance of $r_e(\mathrm{CN}) = 1.1718$ Å.[41] The CN bond length for SiCN is close to r_e(CN) for diatomic CN, while the NC bond distance of SiNC is about 0.02 Å longer. It is seen that correlation effects move some electron density from the electronegative CN (NC) to the electropositive Si for the two radicals.

The predicted rotational constants for SiCN and SiNC

TABLE IV. Theoretical predictions of the total energy (in hartree), dipole moment (in D), harmonic vibrational frequencies (in cm^{-1}), and ZPVE (in kcal mol^{-1}) for the transition state for the isomerization reaction on the $^2A''$ potential energy surface.

Level of theory	Energy	μ_e	$\omega_1(a')$	$\omega_2(a')$	$\omega_3(a')$	ZPVE
TZ2P SCF	−381.177 946	1.958	2315	384*i*	479	3.99
TZ2PF SCF	−381.182 149	1.877	2320	379*i*	483	4.01
cc-pVTZ SCF	−381.184 285	1.850	2316	374*i*	485	4.00
cc-pVQZ SCF	−381.193 389	1.810	2317	376*i*	481	4.00
TZ2P CISD	−381.522 642	1.837	2167	387*i*	485	3.79
TZ2PF CISD	−381.553 248	1.635	2180	385*i*	496	3.83
cc-pVTZ CISD	−381.558 589	1.593	2176	381*i*	500	3.83
cc-pVQZ CISD	−381.587 294	⋯	2188	384*i*	499	3.84
TZ2P CCSD	−381.565 239	1.869	2091	389*i*	480	3.68
TZ2PF CCSD	−381.599 161	1.634	2105	388*i*	493	3.71
cc-pVTZ CCSD	−381.604 955	1.565	2101	384*i*	497	3.71
cc-pVQZ CCSD	−381.635 686	1.464	2113	388*i*	496	3.73
TZ2P CCSD(T)	−381.586 367	1.810	2028	384*i*	478	3.58
TZ2PF CCSD(T)	−381.622 639	1.570	2038	380*i*	491	3.62
cc-pVTZ CCSD(T)	−381.628 819	1.493	2032	378*i*	495	3.61
cc-pVQZ CCSD(T)	−381.661 499	1.464	2046	378*i*	494	3.63
cc-pVTZ CCSDT-3[a]	−381.627 678	⋯	⋯	⋯	⋯	⋯
cc-pVQZ CCSDT-3[a]	−381.660 463	⋯	⋯	⋯	⋯	⋯
cc-pVTZ CCSDT[a]	−381.629 232	⋯	⋯	⋯	⋯	⋯

[a]At the CCSD(T) geometries.

TABLE V. Predicted rotational constants (B_e values) in MHz (in cm^{-1} in parentheses) for the ground states of the SiCN and SiNC molecules.

Molecule	SiCN		SiNC
Level of theory		:	
TZ2P SCF	5493.3(0.183 24)	:	6408.9(0.213 78)
TZ2PF SCF	5507.1(0.183 70)	:	6438.2(0.214 75)
cc-pVTZ SCF	5483.8(0.182 92)	:	6406.3(0.213 69)
cc-pVQZ SCF	5502.9(0.183 56)	:	6435.0(0.214 65)
TZ2P CISD	5472.9(0.182 56)	:	6319.1(0.210 78)
TZ2PF CISD	5504.6(0.183 61)	:	6368.4(0.212 43)
cc-pVTZ CISD	5486.3(0.183 00)	:	6343.2(0.211 59)
cc-pVQZ CISD	5523.0(0.184 23)	:	6391.4(0.213 20)
TZ2P CCSD	5440.1(0.181 46)	:	6273.0(0.209 24)
TZ2PF CCSD	5474.6(0.182 61)	:	6324.8(0.210 97)
cc-pVTZ CCSD	5456.9(0.182 02)	:	6301.1(0.210 18)
cc-pVQZ CCSD	5496.6(0.183 35)	:	6352.1(0.211 88)
TZ2P CCSD(T)	5421.4(0.180 84)	:	6236.0(0.208 01)
TZ2PF CCSD(T)	5458.1(0.182 06)	:	6288.8(0.209 77)
cc-pVTZ CCSD(T)	5440.2(0.181 46)	:	6265.9(0.209 01)
cc-pVQZ CCSD(T)	5480.8(0.182 82)	:	6316.5(0.210 70)
cc-pVTZ CCSDT-3	5440.3(0.181 47)	:	6265.9(0.209 01)
cc-pVQZ CCSDT-3	5480.7(0.182 82)	:	6316.4(0.210 69)
Expt. (Refs. 4 and 5)[a]	5543.4(0.184 91)	:	6396.7(0.213 37)

[a]Experimental values are B_0.

TABLE VII. Relative energies in kcal mol^{-1} (ZPVE corrected values in parentheses) for the SiCN–SiNC system.

Level of theory	SiCN	SiNC	T.S. $^2A'$	T.S. $^2A''$
TZ2P SCF	0.0(0.0)	−3.98(−4.40)	24.14(23.11)	21.80(20.67)
TZ2PF SCF	0.0(0.0)	−5.10(−5.45)	24.65(23.61)	21.88(20.74)
cc-pVTZ SCF	0.0(0.0)	−4.95(−5.31)	24.26(23.23)	21.38(20.24)
cc-pVQZ SCF	0.0(0.0)	−5.28(−5.64)	24.22(23.20)	21.33(20.20)
TZ2P CISD	0.0(0.0)	0.70(0.38)	23.28(22.37)	23.19(22.16)
TZ2PF CISD	0.0(0.0)	−0.24(−0.52)	23.26(22.36)	22.57(21.54)
cc-pVTZ CISD	0.0(0.0)	−0.10(−0.38)	23.13(22.23)	22.31(21.28)
cc-pVQZ CISD	0.0(0.0)	−0.51(−0.79)	23.06(22.17)	22.18(21.15)
TZ2P CCSD	0.0(0.0)	2.22(1.94)	22.77(21.90)	23.80(22.83)
TZ2PF CCSD	0.0(0.0)	1.41(1.18)	22.66(21.82)	23.11(22.14)
cc-pVTZ CCSD	0.0(0.0)	1.51(1.27)	22.57(21.73)	22.87(21.90)
cc-pVQZ CCSD	0.0(0.0)	1.10(0.87)	22.47(21.64)	22.77(21.81)
TZ2P CCSD(T)	0.0(0.0)	2.87(2.62)	21.93(21.11)	23.78(22.86)
TZ2PF CCSD(T)	0.0(0.0)	2.16(1.94)	21.77(20.95)	23.07(22.14)
cc-pVTZ CCSD(T)	0.0(0.0)	2.26(2.04)	21.70(20.89)	22.84(21.91)
cc-pVQZ CCSD(T)	0.0(0.0)	1.86(1.65)	21.56(20.78)	22.73(21.82)
cc-pVTZ CCSDT-3[a]	0.0(0.0)	2.00(1.78)	21.80(20.99)	22.83(21.90)
cc-pVQZ CCSDT-3[a]	0.0(0.0)	1.63(1.42)	21.66(20.88)	22.73(21.82)
cc-pVTZ CCSDT[a]	0.0(0.0)	2.08(1.86)	21.71(20.90)	22.79(21.86)
cc-pVQZ CCSDT[a]	0.0(0.0)	1.69(1.48)	⋯	⋯

[a]At the CCSD(T) geometries.

are presented in Table V. There is a very distinct difference between the rotational constants of the SiCN and SiNC molecules. The trends in theoretical rotational constants are reasonably consistent with respect to correlation effects and basis set expansion. The CCSD(T) and CCSDT-3 methods (both include triple excitations) provide practically identical rotational constants. At the cc-pVQZ CCSDT-3 level of theory the equilibrium rotational constants (B_e values) are determined to be 5480.7 MHz (0.182 82 cm^{-1}) for SiCN and 6316.4 MHz (0.210 69 cm^{-1}) for SiNC. These predictions are in good accord with the experimental rotational constants (B_0 values) of 5543.4 MHz (0.184 91 cm^{-1}) for SiCN and 6396.7 MHz (0.213 37 cm^{-1}) for SiNC.[4,5] The theoretical B_e values at the less complete SCF and CISD levels of theory are fortuitously close to the experimental B_0 values.

TABLE VI. The predicted Renner parameters (ϵ) and averaged harmonic bending vibrational frequencies ($\tilde{\omega}_2$) in cm^{-1} for the $^2\Pi$ ground states of SiCN and SiNC.

Molecule	SiCN	SiCN	SiNC	SiNC
Level of theory	ϵ	$\tilde{\omega}_2$	ϵ	$\tilde{\omega}_2$
TZ2P SCF	0.273	279	0.385	186
TZ2PF SCF	0.270	287	0.307	213
cc-pVTZ SCF	0.268	285	0.312	209
cc-pVQZ SCF	0.277	282	0.321	206
Mean SCF values	0.272	283	0.331	204
TZ2P CISD	0.280	262	0.400	191
TZ2PF CISD	0.287	265	0.358	206
cc-pVTZ CISD	0.284	265	0.367	204
cc-pVQZ CISD	0.301	263	0.383	202
Mean CISD values	0.288	264	0.377	201
TZ2P CCSD	0.287	255	0.420	190
TZ2PF CCSD	0.296	257	0.386	203
cc-pVTZ CCSD	0.294	256	0.395	201
cc-pVQZ CCSD	0.307	255	0.415	200
Mean CCSD values	0.296	256	0.404	199
TZ2P CCSD(T)	0.305	246	0.423	187
TZ2PF CCSD(T)	0.309	253	0.401	200
cc-pVTZ CCSD(T)	0.327	250	0.401	198
cc-pVQZ CCSD(T)	0.329	245	0.423	196
Mean CCSD(T) values	0.318	249	0.412	195

The transition state structures for the isomerization reaction on the $^2A'$ surface are shown in Fig. 5 and those on the $^2A''$ surface are shown in Fig. 6. The $^2A'$ transition state has not been considered in previous research. Although the CN bond lengths are similar for the two transition states, the SiCN bond angles are quite different. The transition state on the $^2A'$ surface has a SiCN bond angle of around 97° which is significantly closer to the reactant (SiCN) structure. On the contrary, on the $^2A''$ surface the transition state is somewhat shifted toward the product (SiNC) structure with a SiCN bond angle of around 72°. The CN bond lengths are lengthened with advanced treatments of correlation effects. At each correlated level of theory, the CN bond distances for the two transition states range between the CN bond length of SiCN and the NC bond length of SiNC at their equilibrium.

B. Dipole moments

The dipole moment of the linear SiCN molecule generally decreases with increasing basis set size and more sophisticated treatments of correlation effects. On the other hand, the dipole moment of the linear SiNC species generally increases with advanced correlation effects and decreases with basis set size. The dipole moments of SiCN and SiNC are

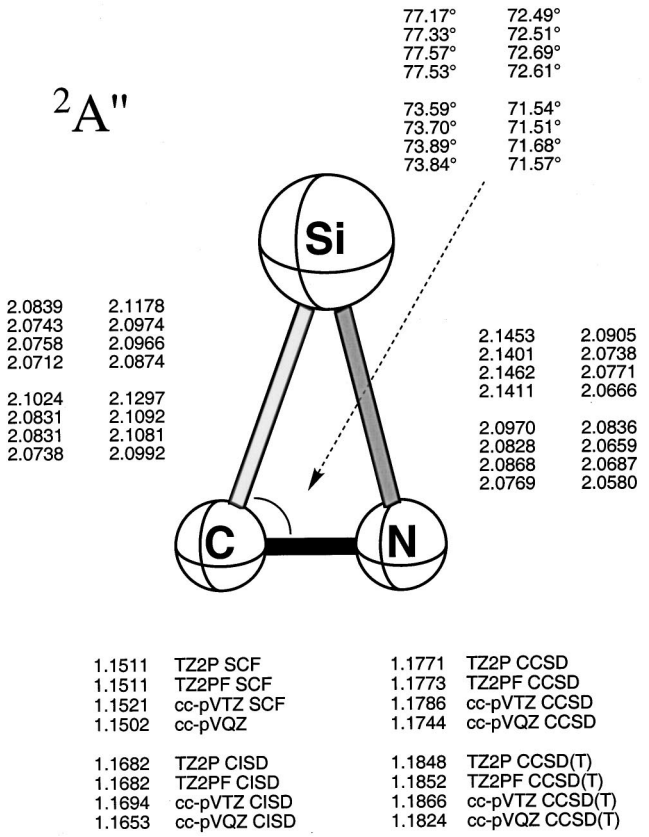

FIG. 6. Predicted geometries for the $^2A''$ transition state for the SiCN↔SiNC isomerization reaction. Bond lengths are in Å.

predicted to be 3.09 and 2.65 Debye, respectively, at the cc-pVQZ CCSD(T) level of theory. The directions of the dipole moments are predicted to be $^+SiCN^-$ and $^+SiNC^-$ for the two linear isomers. In their earlier paper in 2000 Apponi *et al.*[4] suggested that due to its larger dipole moment and by analogy with the known metal cyanides already observed toward IRC +10216, SiCN was the most likely of the three molecules (SiCCH, SiCN, and SiNC) to be found in space. Only a few months later they indeed detected the SiCN radical in an astronomical source.[6]

For the two transition states, the dipole moments usually decrease with advanced treatments of correlation effects and basis set expansion. The dipole moments of the two transition states are smaller in magnitude than those of the reactant and product. The $^2A'$ transition state has a larger dipole moment than the $^2A''$ transition state. Since the components of dipole moments are nonvanishing only in the molecular plane, shifting the electron density from the $12a'$ (in-plane) MO to the $3a''$ (out-of-plane) MO appears to diminish the polarity of these structures.

C. Vibrational frequencies

The CN stretching frequency (ω_1) for SiCN in Table I decreases with treatment of correlation effects, reflecting the elongated CN bond distance. The NC stretching frequency (ω_1) for SiNC in Table II also decreases with advanced treatment of correlation effects. Reflecting the longer NC bond for SiNC, the NC stretching frequency of SiNC is lower than the CN stretching frequency of SiCN. The experimental[41] harmonic vibrational frequency of the diatomic $X\,^2\Sigma^+$ CN is 2068.6 cm^{-1}. The CN stretching frequency of SiCN is higher than the diatomic frequency, whereas the NC stretching frequency of SiNC is lower than the diatomic frequency. Therefore, the multiple bond character of NC in SiNC appears to be less than that of CN in SiCN. The SiC stretching frequency (ω_3) of SiCN is insensitive to correlation effects, reflecting the smaller changes in the SiC bond length. The SiN stretching frequency (ω_3) of SiNC slightly decreases with improved descriptions of correlation effects. Since the SiN stretching frequency of SiNC is considerably higher than the SiC stretching frequency of SiCN, it may reasonably be concluded that the Si—NC bond is stronger than the Si—CN bond.

The imaginary vibrational frequencies for the two reaction coordinates (ω_2) have similar magnitudes. The CN stretching (ω_1) frequency for the $^2A''$ transition state is somewhat higher than the CN stretching frequency of the $^2A'$ transition state, reflecting slightly shorter CN bond distance. These two CN stretching frequencies are decreased as the treatment of correlation effects becomes more complete. Furthermore, at each level of theory, these transition state frequencies range between the CN stretching frequency of SiCN and the NC stretching frequency of SiNC.

D. Renner–Teller effect

The Renner parameters and averaged harmonic bending frequencies for SiCN and SiNC are presented in Table VI. The Renner parameters for the two linear radicals increase with more complete treatments of correlation effects, while the averaged bending frequencies decrease. The mean values of these two quantities for $\tilde{X}\,^2\Pi$ SiCN are $\epsilon=0.318$ and $\tilde{\omega}_2=249\ cm^{-1}$ at the CCSD(T) level of theory. The corresponding values for the $\tilde{X}\,^2\Pi$ ground state of SiNC are predicted to be $\epsilon=0.412$ and $\tilde{\omega}_2=195\ cm^{-1}$ with the same method. The SiNC molecule presents a larger Renner parameter than the SiCN molecule, whereas the SiCN species has the higher averaged bending frequency.

E. Energetics

Relative energies for the four stationary points investigated in this research are shown in Table VII. Using the cc-pVQZ basis set, the classical energy differences between the SiCN and SiNC isomers are −5.28 (SCF), −0.51 (CISD), 1.10 (CCSD), 1.86 [CCSD(T)], 1.63 (CCSDT-3), and 1.69 kcal/mol (CCSDT). The SCF wave functions predict SiNC to lie below SiCN, while the CISD wave functions predict the two isomers to be almost isoenergetic. On the other hand, the more complete CCSD, CCSD(T), CCSDT-3, and CCSDT levels of theory indicate SiCN to lie below SiNC. In our experience, the wave functions including higher excitations favorably stabilize isomers with multiple bonds. The SiCN radical with a CN bond of greater multiple bond character may be preferably stabilized compared to the SiNC radical with a NC bond of lesser multiple bond character. At the cc-pVQZ CCSDT level of theory the SiCN radical is predicted to lie 1.48 kcal/mol (including the ZPVE

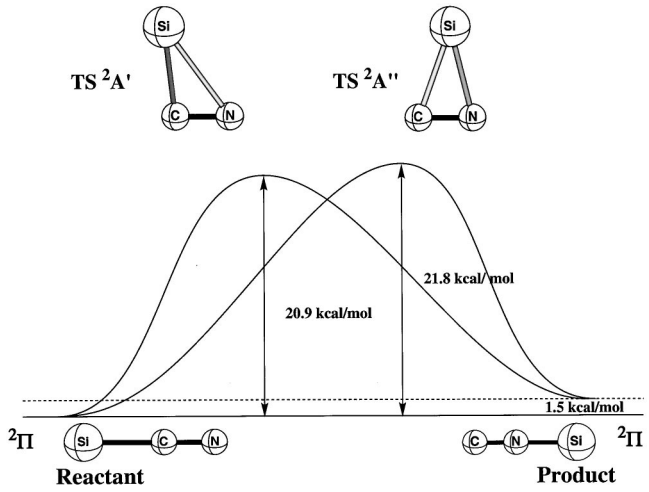

FIG. 7. Schematic potential energy surfaces for the SiCN–SiNC system.

corrections) lower in energy than the SiNC isomer. Largo-Cabrerizo made a very reasonable prediction of this energy difference to be 1.9 kcal/mol at the MP4 (SDTQ)/MC-311G(d)//UHF/6-31G(d) level of theory.[3]

The transition state on the $^2A'$ surface is located 24.2 (SCF), 23.1 (CISD), 22.5 (CCSD), 21.6 [CCSD(T)], and 21.7 kcal/mol (CCSDT-3) above the SiCN ground state. The $^2A'$ barrier height decreases with correlation effects. On the $^2A''$ surface the transition state lies 21.3 (SCF), 22.2 (CISD), 22.8 (CCSD), 22.7 [CCSD(T)], and 22.7 kcal/mol (CCSDT-3) above the SiCN ground state. Largo-Cabrerizo located the $^2A''$ transition state 21.3 kcal/mol above the SiCN isomer (19.0 kcal/mol above the SiNC isomer) at the MP2/6-31G(d)//UHF/6-31G(d) level of theory.[3] The $^2A''$ activation energy increases with advanced treatments of correlation effects. The transition state on the $^2A''$ surface is located *below* the transition state on the $^2A'$ surface at the SCF and CISD levels of theory. This situation is reversed with the CC methods: The transition state on the $^2A''$ surface lies *above* the transition state on the $^2A'$ surface.

At the $^2A''$ transition state, there is an empty orbital ($12a'$) on the Si atom and a lone pair on the N atom that serve to form a cyclic structure and to stabilize the transition state. With the SCF method the more nearly isosceles $^2A''$ transition state is indeed stabilized as much as 3 kcal/mol relative to the L-shaped $^2A'$ transition state. However, higher excitations appear to stabilize preferentially the L-shaped $^2A'$ transition structure. With the ZPVE corrections the barriers on the $^2A'$ and $^2A''$ surfaces are determined to be 20.9 and 21.8 kcal/mol above the SiCN isomer at the cc-pVQZ CCSDT-3 level of theory. The potential energy surfaces are schematically depicted in Fig. 7. As discussed in Sec. II, at the $^2A'$ transition state geometry there exists the lower-lying $^2A''$ state, while at the $^2A''$ transition state geometry there is the lower-lying $^2A'$ state. Since the activation energies are considerable, the SiCN↔SiNC isomerization reaction will not occur readily in interstellar space.

VI. CONCLUDING REMARKS

Employing *ab initio* electronic structure theory, the ground states of the silicon cyanide (SiCN) and silicon isocyanide (SiNC) molecules have been investigated. With the cc-pVQZ CCSDT method (including *all* triple excitations) at the CCSD(T) optimized geometries SiCN is predicted to be 1.5 kcal/mol lower in energy than SiNC. The theoretical B_e values of 5481 MHz (SiCN) and 6316 MHz (SiNC) at the cc-pVQZ CCSDT-3 level of theory are in good accord with the experimental B_0 values of 5543 MHz (SiCN) and 6397 MHz (SiNC). The Renner parameters and averaged harmonic bending frequencies of $\tilde{X}\,^2\Pi$ states were predicted to be 0.318 and 249 cm^{-1} for SiCN and 0.412 and 195 cm^{-1} for SiNC. Transition states for the isomerization reaction (SiCN→SiNC) have been located on both the $^2A'$ and $^2A''$ surfaces. The $^2A'$ transition state is predicted to lie 20.9 kcal/mol above the ground state of SiCN, while the $^2A''$ transition state is located slightly higher, at 21.8 kcal/mol above the ground state of SiCN.

ACKNOWLEDGMENTS

The authors would like to thank Professor Nicholas C. Handy for helpful discussions and Kurt W. Sattelmeyer for his expertise. This research was supported by the U.S. National Science Foundation, Grant No. CHE-0136186.

[1] M. Guélin, J. Cernicharo, C. Kahone, and J. Gomez-Gonzalez, Astron. Astrophys. **157**, L17 (1986).
[2] A. Largo-Cabrerizo and J. R. Flores, Chem. Phys. Lett. **146**, 90 (1998).
[3] A. Largo-Cabrerizo, Chem. Phys. Lett. **147**, 95 (1998).
[4] A. J. Apponi, M. C. McCarthy, C. A. Gottlieb, and P. Thaddeus, Astrophys. J. **536**, L55 (2000).
[5] M. C. McCarthy, A. J. Apponi, C. A. Gottlieb, and P. Thaddeus, J. Chem. Phys. **115**, 870 (2001).
[6] M. Guélin, S. Muller, J. Cernicharo, A. J. Apponi, M. C. McCarthy, C. A. Gottlieb, and P. Thaddeus, Astron. Astrophys. **363**, L9 (2000).
[7] G. D. Purvis and R. J. Bartlett, J. Chem. Phys. **76**, 1910 (1982).
[8] M. Rittby and R. J. Bartlett, J. Phys. Chem. **92**, 3033 (1988).
[9] K. Raghavachari, G. W. Trucks, J. A. Pople, and M. Head-Gordon, Chem. Phys. Lett. **157**, 479 (1989).
[10] G. E. Scuseria, Chem. Phys. Lett. **176**, 27 (1991).
[11] J. Noga, R. J. Bartlett, and M. Urban, Chem. Phys. Lett. **134**, 126 (1987).
[12] J. Noga and R. J. Bartlett, J. Chem. Phys. **86**, 7041 (1987).
[13] G. E. Scuseria and H. F. Schaefer, Chem. Phys. Lett. **152**, 382 (1988).
[14] J. D. Watts and R. J. Bartlett, J. Chem. Phys. **93**, 6104 (1990).
[15] A. D. Walsh, J. Chem. Soc. **1953**, 2288.
[16] G. Herzberg and E. Teller, Z. Phys. Chem. Abt. B **21**, 410 (1933).
[17] R. Renner, Z. Phys. **92**, 172 (1934).
[18] J. T. Hougen, J. Chem. Phys. **36**, 1874 (1961).
[19] G. Herzberg, *Molecular Spectra and Molecular Structure*, Vol. III, Electronic Spectra and Electronic Structure of Polyatomic Molecules (Van Nostrand, Princeton, 1966).
[20] Ch. Jungen and A. J. Merer, in *Molecular Spectroscopy: Modern Research*, edited by K. N. Rao (Academic, New York, 1976), Vol. 2, pp. 127–164.
[21] J. M. Brown and F. Jørgensen, Adv. Chem. Phys. **52**, 117 (1983).
[22] T. J. Lee, D. J. Fox, H. F. Schaefer, and R. M. Pitzer, J. Chem. Phys. **81**, 356 (1984).
[23] P. R. Bunker and P. Jensen, *Molecular Symmetry and Spectroscopy*, 2nd ed. (NRC Research, Ottawa, 1998).
[24] P. Jensen, G. Osmann, and P. R. Bunker, in *Computational Molecular Spectroscopy*, edited by P. Jensen and P. R. Bunker (Wiley, Chichester, 2000), pp. 485–515.
[25] J. M. Brown, in *Computational Molecular Spectroscopy*, edited by P. Jensen and P. R. Bunker (Wiley, Chichester, 2000), pp. 517–537.
[26] L. Pauling, *The Nature of the Chemical Bond*, 3rd ed. (Cornell University Press, New York, 1960).

[27] Y. Yamaguchi, I. L. Alberts, J. D. Goddard, and H. F. Schaefer, Chem. Phys. **147**, 309 (1990) and references therein.
[28] N. A. Burton, Y. Yamaguchi, I. L. Alberts, and H. F. Schaefer, J. Chem. Phys. **95**, 7466 (1991).
[29] T. D. Crawford, J. F. Stanton, W. D. Allen, and H. F. Schaefer, J. Chem. Phys. **107**, 10626 (1997).
[30] T. H. Dunning, J. Chem. Phys. **55**, 716 (1971).
[31] S. Huzinaga, J. Chem. Phys. **42**, 1293 (1965).
[32] A. D. McLean and G. S. Chandler, J. Chem. Phys. **72**, 5639 (1980).
[33] S. Huzinaga, *Approximate Atomic Functions II*, Department of Chemsitry Report, University of Alberta, Edmonton, Alberta, Canada, 1971.
[34] T. H. Dunning, J. Chem. Phys. **90**, 1007 (1989).
[35] D. E. Woon and T. H. Dunning, J. Chem. Phys. **98**, 1358 (1993).
[36] P. Pulay, Mol. Phys. **17**, 197 (1969).
[37] P. Pulay, in *Modern Theoretical Chemistry*, edited by H. F. Schaefer (Plenum, New York, 1977), Vol. 4, pp. 153–185.
[38] Y. Yamaguchi, Y. Osamura, J. D. Goddard, and H. F. Schaefer, *A New Dimension to Quantum Chemistry: Analytic Derivative Methods in Ab Initio Molecular Electronic Structure Theory* (Oxford University Press, New York, 1994).
[39] PSI 2.0.8; C. L. Janssen, E. T. Seidl, G. E. Scuseria *et al.*, PSITECH, Inc., Watkinsville, GA, 30677, 1994.
[40] ACES II: J. F. Stanton, J. Gauss, W. J. Lauderdale, J. D. Watts, and R. J. Bartlett. The package also contains modified versions of the MOLECULE Gaussian integral program of J. Almlöf and P. R. Taylor, the ABACUS integral derivative program written by T. U. Helgaker, H. J. Aa. Jensen, P. Jørgensen, and P. R. Taylor, and the PROPS property evaluation integral code of P. R. Taylor.
[41] K. P. Huber and G. Herzberg, *Molecular Spectra and Molecular Structure*, Vol. IV, Constants of Diatomic Molecules (Van Nostrand Reinhold, New York, 1979).